Inorg. Chem. **2003**, *42*, 4088–4097

An Average-of-Configuration Method for Using Kohn–Sham Density Functional Theory in Modeling Ligand-Field Theory†

Christian Anthon,‡ Jesper Bendix,§ and Claus E. Schäffer*

Department of Chemistry, Chemical Laboratory I, H. C. Ørsted Institute, University of Copenhagen, Universitetsparken 5, DK-2100 Copenhagen, Denmark

Received November 28, 2002

The Amsterdam Density Functional (ADF) package has been used to constrain Kohn–Sham DFT in such a fashion that a transition from KS-DFT to ligand-field theory in the form of the parametrical d^q model is completely well-defined. A relationship is established between the strong-field approximation of the parametrical d^2 model for the tetrahedral complexes VCl_4^- and VBr_4^- and certain fixed-orbital ADF-computed energies. In this way values for all the parameters of the d^2 model may be computed, thus allowing the ADF results to be expressed in terms of a KS-DFT energy matrix that can be diagonalized. This means that the KS-DFT deficiency with regard to computation of nondiagonal elements has been overcome and the KS-DFT eigenenergies have become available through the KS-DFT mimicking of the ligand-field plus repulsion model. By using mutually orthogonal strong-field energy matrices, the mimicking has been further elucidated. The computed values for the empirical parameters of VCl_4^- and VBr_4^- are in good agreement with experimental data. The spectrochemical and the nephelauxetic series have been computed by including the remaining halide complexes and the quantitatively special position of F^- among the halides corroborated for both series.

1. Introduction

Ligand-field theory revolutionized the conceptual part of classical transition metal chemistry 40 years ago.[1] However, there is still a need for elucidating the parameters of this model theory by a systematic and transparent method of computation of their numerical values. Our ambition here is to describe such a method. Our method was designed to provide qualitative insight, but it turned out to provide valuable numerical information as well.

Historically the parametrical d^q model was based upon the electrostatic model in which the ligands perturbed the central ion by virtue of the electrical charges or dipoles they carried.[2,3] The interelectronic repulsion between the electrons of the central ion was not expected to change under the influence of ligands modeled in this way. However, when the parametrical d^q model was used semiempirically, the empirical values of the interelectronic repulsion parameters found for complexes were invariably lower than those of the corresponding gaseous ions.[4] This fact was taken as evidence of covalency of the bonds between the metal ions and their ligands. It was explained mainly by an invasion of charge from the ligands into the central ion region, thereby causing a screening of the d electrons from the nucleus (central field covalency). The concurring radial expansion of the d orbitals was named nephelauxetism or cloud expansion of the partially filled shell.[4] This conceptual interpretation made the basis for the naming of the expanded radial function model.[4c] An alternative qualitative explanation[4c] of the phenomenon of nephelauxetism could be given in a linear combination of atomic orbitals molecular orbital (LCAO-MO) vocabulary where the eigenorbitals of the partially filled shell would contain d-character in a diluted form being a linear combination of d orbitals and symmetry-adapted ligand orbitals (symmetry-restricted covalency). With

* Corresponding author. E-mail: ces@kiku.dk.

† Communicated in part at the 35th Conference on Coordination Chemistry, Heidelberg 2002.

‡ E-mail: anthon@kiku.dk.

§ E-mail: bendix@kiku.dk.

(1) Jørgensen, C. K. *Absorption Spectra and Chemical Bonding*: Academic Press: New York, 1962.

(2) Ballhausen, C. J. *Introduction to ligand field theory*: McGraw-Hill: New York, 1962.

(3) Griffith, J. S. *The Theory of Transition-Metal Ions*: Cambridge University Press: Cambridge, 1961.

(4) (a) Schäffer, C. E.; Jørgensen, C. K. *J. Inorg. Nucl. Chem.* **1958**, *8*, 143 (Reprinted in: *Symmetry in Chemical Theory*; Fackler, J. P., Ed.; Dowden, Hutchinson & Ross: Stroudsberg, PA, 1973.) (b) Schäffer, C. E. *Ibid.* **1958**, *8*, 149. (c) Jørgensen, C. K *Prog. Inorg. Chem.* **1962**, *4*, 73.

10.1021/ic0262233 CCC: $25.00 © 2003 American Chemical Society
Published on Web 05/23/2003

the work using the present method, we hope eventually to become able to cast new light upon these cooperating covalencies and in particular to be able to associate these with the nephelauxetic series of ligands.[4]

Density functional theory (DFT) has invaded chemistry with considerable impact. Commercially available program packages[5,6a] using Kohn−Sham DFT may already be considered to be one of chemistry's standard tools.[7] As far as we are concerned, it is the fact that KS-DFT is an orbital model which has attracted us by the perspective of making it commensurable with the parametrical d^q model.

Some efforts in the direction of obtaining a correspondence between DFT and LFT focused on the ligand field itself by attempting to achieve commensurable orbital splitting patterns by the two methods.[8] The interelectronic repulsion part of LFT could be included by using the suggestion of Ziegler et al.,[9] in which the energies of many electron eigenfunctions are written as linear combinations of those of single Slater determinantal functions. Through these Slater determinants an approximate 1:1 correspondence with KS-DFT was suggested, allowing their energy expectation values to be computed.[9] Thus, if—for a given electron configuration—the number of determinants that are associated with different energies is equal to or greater than the number of eigenenergies, these can be calculated by solving a system of simultaneous linear equations. Unfortunately, the devised method turned out to have limitations that were illustrated[9] by an example using symmetry: the first excited configuration of benzene is of the type $e_1e_2(D_6)$ giving the six states $^{3,1}B_1$, $^{3,1}B_2$, $^{3,1}E$ but only four determinants of different energies. Daul[10] developed and used[11] this suggestion by applying the method of irreducible tensor operators and proposed to use a number of Slater determinants equal to the number of so-called reduced matrix elements, which are the parameters to be determined. Any remaining Slater determinants were described as redundant. This proposal suffers from an arbitrary selection of the Slater determinants used and thereby the risk of incorporating systematic errors of the KS-DFT in the parametric results.

In order to circumvent this arbitrariness and in order to be able to analyze in more detail the strengths and shortcomings in the DFT modeling of LFT, we have recently introduced an intermediate step where we use the complete set of Slater determinants and reduce their calculated energies to multiplet term energies by solving an overcomplete set of linear equations. The use of real orbitals circumvented certain symmetry problems of KS-DFT.

We have demonstrated this method by using the ADF package to compute successfully a set of Slater−Condon−Shortley (SCS) parameters of interelectronic repulsion referring to atomic d^q ions.[12] The method used for these atomic computations conserved the concepts of ligand-field theory apart from the fact that we only reached the stage of zero ligand field. This approach has now been developed so as to make it in principle applicable to ligand-field systems, and we demonstrate this usage here.[13] We are particularly focusing on the phenomenon of nephelauxetism, which has only been experimentally quantified for systems with orbitally nondegenerate ground states. Tetrahedral VCl_4^- is an example of such a system.

This ion was predicted by ligand-field theory to have a ground state $^3A_2(T_d)$ belonging to the half-filled subconfiguration, $[e(T_d)]^2$. Since the ligand field is barycentered, this configuration gives rise to a maximal ligand-field stabilization for a tetracoordinated d^q system. The ion was subsequently prepared and isolated in the form of its tetraethylammonium salt.[14a] This complex and its homologous complexes with the other halides will be used here as an illustration of our method.

2. The Parametrical d^q Model

Ligand-field theory of d electrons is a model theory concerned with energy differences between the states of the partially filled d shell, which can be classified as having a parentage of mainly a d^q configuration of the central ion. This classifying d^q configuration was named the preponderant configuration by Jørgensen.[15] For $2 \leq q \leq 8$ the ligand-field model embodies a one-electron term called the ligand field, LF, and a two-electron term representing the interelectronic repulsion, R, within the partially filled shell. The two terms are expressed semiempirically, that is, in energy parameters whose values are determined by comparison of theory and experiment. These empirical parameters of the combined ligand-field plus repulsion model, LFR, will be computed here by the ADF.

In most formulations the one-electron and two-electron terms have their own zero points of energy, which cannot be separated or otherwise elucidated or determined by the

(5) Gaussian, program documentation available at http://www.gaussian.com.

(6) (a) ADF2000 program documentation available at http://www.scm-.com. (b) Baerends, E. J.; Ellis, D. E.; Ros, P. *Chem. Phys.* **1973**, *2*, 41. (c) Versluis, L.; Ziegler, T. *J. Chem. Phys.* **1988**, *88*, 322. (d) te Velde, G.; Baerends, E. J. *J Comput. Phys.* **1992**, *99* (1), 84. (e) Fonseca Guerra, C.; Snijders, J. G.; te Velde, G.; Baerends, E. J. *Theor. Chem. Acc.* **1998**, *99*, 391.

(7) (a) Chermette, H. *Coord. Chem. Rev.* **1998**, *178−180*, 699. (b) Deeth, R. J. *Struct. Bonding* **1995**, *82*, 1.

(8) (a) Deeth, R. J. *J. Chem. Soc., Dalton Trans.* **1991**, 1467. (b) Deeth, R. J. *J. Chem. Soc., Dalton Trans.* **1990**, 365. (c) Woolley, R. G., *Int. Rev. Phys. Chem*. **1987**, *6*, 93. (d) Woolley, R. G. *Philos. Mag. B* **1994**, *69*, 745.

(9) Ziegler, T.; Rauk, A, Baerends, E. J. *Theor. Chim. Acta* **1977**, *43*, 261.

(10) Daul, C. *Int. J. Quantum Chem.* **1994**, *52*, 867.

(11) (a) Daul, C. A.; Güdel, H.-U.; Weber, J. *J. Chem. Phys.* **1993**, *98*, 4023. (b) Daul, C. A.; Doclo, K. G.; Stückl, A. C. *Recent Advances in Density Functional Methods, Part II*; World Scientific Publishing Company: Singapore, 1997. (c) Mineva, T.; Goursot, A.; Daul, C. *Chem. Phys. Lett.* **2001**, *350*, 147.

(12) Anthon, C.; Schäffer, C. E. *Coord. Chem. Rev.* **2002**, *226*, 17.

(13) After the submission of this manuscript a paper by Atanasov et. al. (Atanasov, M.; Daul, C. A.; Rauzy, C. *Chem. Phys. Lett.* **2003**, *367*, 737) has appeared, which employs the usage of an overcomplete set of determinantal energies as described in ref 12. That paper has a different focus than the present one and investigates different chemical systems.

(14) (a) Scaife, D. E. *Chem. Soc. Spec. Publ.* **1959**, No. 13, p 152. (b) Gruen, D. M.; Gut, R. *Nature* **1961**, *190*, 713. (c) Clark, R. J. H.; Nyholm, R. S.; Scaife, D. E. *J. Chem. Soc. A* **1966**, 1296. (d) Casey, A. T.; Clark, R. J. H. *Inorg. Chem.* **1968**, *7*, 1598. (e) Scaife, D. E. *Aust. J. Chem.* **1970**, *23*, 2205.

(15) Jørgensen, C. K. *Oxidation numbers and oxidation states*: Springer Verlag: Berlin, 1969.

comparison with experiments.[1] It is possible to eliminate these zero point problems by barycentration,[16,17,18c] that is, by isolating the average energy of all the states under consideration. Thus the Hamiltonian can be written as

$$\hat{H}_{\mathrm{LFR}} = \hat{H}_{\mathrm{LF}} + \hat{H}_{\mathrm{R}} = H_{\mathrm{av}}\hat{1} + \hat{\bar{H}}_{\mathrm{LF}} + \hat{\bar{H}}_{\mathrm{R}} = H_{\mathrm{av}}\hat{1} + \hat{\bar{H}}_{\mathrm{LFR}} \quad (1)$$

where $\hat{H}_{\mathrm{LFR}}$ acts on the so-called d^q configuration or a subspace thereof. In the present paper we shall discuss the d^2 configuration and restrict ourselves to the subspace consisting of the 10 states with $M_S = S = 1$, that is, the $M_S = 1$ states whose central ion parentages are the $M_S = 1$ components of the multiplet terms ^{3}P and ^{3}F. Moreover, we shall only discuss tetrahedral complexes of the type VX_4^- with V^{III} as the central ion. These restrictions do not in any way prevent us from describing our method, but they do simplify our presentation. Thus, we have obtained a situation where we are left with one ligand-field parameter Δ and one repulsion parameter, the Racah parameter B, which we shall denote by B^1 here, 1 referring to $S = 1$. The definitions of the parameters are illustrated in a and b:

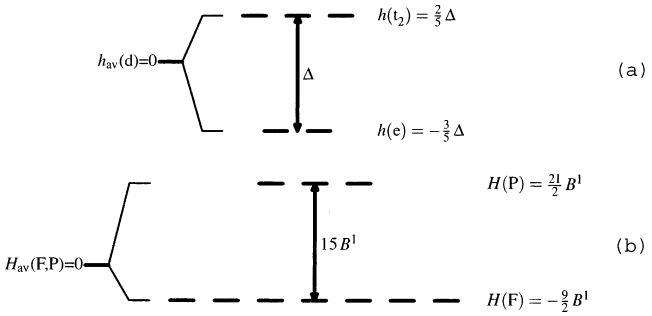

In these circumstances the parametrical d^q model can be written as a sum of conglomerate operators,[12,16,17] each of which is a product of a parameter and its associated coefficient operator

$$\hat{\bar{H}}_{\mathrm{LFR}} = H_{\mathrm{av}}\hat{1} + \Delta\hat{\bar{H}}_{\Delta} + B^1\hat{\bar{H}}_{B^1}$$
$$\hat{\bar{H}}_{\mathrm{LFR}} = \Delta\hat{\bar{H}}_{\Delta} + B^1\hat{\bar{H}}_{B^1} \quad (2)$$

where the coefficient operators $\hat{\bar{Q}}_{\Delta}$ and $\hat{\bar{Q}}_{\mathrm{B}}{}^1$ are barycentered and mutually orthogonal. $\hat{1}$ is the operator whose matrix is a unit matrix in any orthogonal function basis. The concept of orthogonality derives from the idea of a scalar product (or overlap)[18] of a pair of operators $\hat{A}$ and $\hat{B}$, which for real matrices are defined by

$$\langle\hat{A}|\hat{B}\rangle = \sum_{i,j}\mathbf{A}_{ij}\mathbf{B}_{ij} \quad (3)$$

The value is independent of the function basis in which the matrices are set up. Equation 3 provides analogies on the one hand between vectors and operators, and on the other hand between vectors and the matrices of these operators in any fixed basis. This vector/operator analogy has been used before to quantify parametrical ligand-field theory,[12,16] and the vector/matrix analogy will be used in section 4 to illustrate our present method of mimicking LFR by ADF.

The fact that only energy differences are observable as empirical parameters of ligand-field theory is often built into the model by barycentration, in which case the weighted sum of the energies of the complete set of d^q states equals zero.[19] The same applies, of course, to their weighted average energy. A measure of the average energy splitting of the d^q configuration may then be taken as the root-mean-square splitting. The weighted sum of the squares of the eigenenergies of all the barycentered states has been called the sum square splitting (SSS).[16]

The SSS is closely related to the overlap of eq 3. In fact, it is the self-overlap of the barycentered Hamiltonian. For any fitted model describing the experiment, the modeled sum-square splitting will be lower than the experimental one.[19] Furthermore, if the model is a sum of orthogonal operators like in eq 2, the sum-square splitting is a sum of contributions from the individual parameters:

$$\mathrm{SSS}_{\mathrm{exp}} > \mathrm{SSS}_{\mathrm{model}} = (B^1)^2\langle\hat{\bar{Q}}_{B^1}|\hat{\bar{Q}}_{B^1}\rangle + \Delta^2\langle\hat{\bar{Q}}_{\Delta}|\hat{\bar{Q}}_{\Delta}\rangle \quad (4)$$

that is, not containing cross products of parameters.

3. Constraining Kohn−Sham DFT

KS-DFT must, when used for mimicking LFR, treat all the states of the partially filled shell on an equal footing. This implies that each complex imposes an average of configuration reference state of its own and thus each complex imposes different constraints on the KS-DFT. Because of these constraints KS-DFT cannot be applied energetically optimally when the aim is to simulate an LFR description.

All the calculations presented here were done with the 2002.01 version of the ADF package using the triple-ζ basis sets with two polarization functions for vanadium but only one polarization function for the halides. These choices solved the SCF convergence problems in the simpler basis sets and gave the correct ordering of the complexes in the nephelauxetic series. The gradient-corrected functional PW91 was used,[20] since the uncorrected ones (LDA) were previously found to treat the interelectronic repulsion less convincingly.[12] In the iodine basis set the orbitals are unfrozen only from above 4s. For reasons of analysis the fragments were chosen as vanadium(III) and halide anions.

(16) Bendix, J.; Brorson, M.; Schäffer, C. E. In *Oxidation states and d^q configurations in inorganic chemistry*; Kauffman, G. B., Ed.; ACS Symposium Series 565; American Chemical Society: Washington, DC, 1994; p 213.
(17) (a) Schäffer, C. E. *Inorg. Chim. Acta* **2000**, *300*, 1053. (b) Schäffer, C. E. *Struct. Bonding* **1973**, *14*, 69. (c) Schäffer, C. E. In *Wave Mechanics−the first 50 years*; Price, W. C., Chissick, S. S., Ravensdale, T., Eds.; Butterworth: London, 1973; Chapter 12.
(18) (a) Schäffer, C. E. *Physica A (Amsterdam)* **1982**, *114A*, 28. (b) Brorson, M.; Damhus T.; Schäffer, C. E. *Comments Inorg. Chem.* **1983**, *3*, 1. (c) Brorson, M.; Schäffer, C. E. *Inorg. Chem.* **1988**, *27*, 2522.
(19) Bendix, J.; Brorson, M.; Schäffer, C. E. *Inorg. Chem.* **1993**, *32*, 2838.
(20) Perdew, J. P.; Chevary, J. A.; Vosko, S. H.; Jackson, K. A.; Pederson, M. R.; Singh, D. J.; Fiolhais, C. *Phys. Rev. B* **1992**, *46*, 6671.

Table 1. Slater Determinants for One Representative Component of Each of the Four Tetrahedral Spin Triplet d^2 Strong-Field Terms, and Their ADF Energies for VCl_4^- [a]

Sub-configuration	Slater determinant	Symmetry	Contents (LFT)	ADF energy
t_2^2	$\lvert^{+}_{(zx)}\ ^{+}_{(yz)}\rvert$	$^3T_1\,z$	80% ^3F + 20% ^3P	−0.190 μm^{-1}
et_2	$\lvert^{+}_{(x^2-y^2)}\ ^{+}_{(xy)}\rvert$	$^3T_1\,z$	20% ^3F + 80% ^3P	−0.282 μm^{-1}
et_2	$\lvert^{+}_{(z^2)}\ ^{+}_{(xy)}\rvert$	$^3T_2\,xy$	^3F	−0.859 μm^{-1}
e^2	$\lvert^{+}_{(z^2)}\ ^{+}_{(x^2-y^2)}\rvert$	$^3A_2$	^3F	−1.384 μm^{-1}

[a] The energy difference between the et_2 multiplets $^3T_1$ and $^3T_2$ is 80% of $15B^1$, i.e., $12B^1$, and that between $^3T_2$ (et_2) and $^3A_2$ (e^2) is Δ, giving $B^1 = 0.0481$ μm^{-1} and $\Delta = 0.525$ μm^{-1}, respectively. These values are close to the least-squares values of Table 3. The zero point of energy is that of the d^q-AOC-SCF computation. Note that the lower-energy $^3T_1$ is that containing most of the upper-energy term (^3P) in agreement with the fact that the multiplet terms of the gaseous ion are 80% mixed in the strong-field limit (strong-field approximation).

Table 2. Linking the Computed ADF-Model Energies with the LFR Parameters[a]

Slater determinant	Pair-energy class	H_{LFR}	H_{ADF}
$\lvert^{+}_{(zx)}\ ^{+}_{(xy)}\rvert$, $\lvert^{+}_{(zx)}\ ^{+}_{(yz)}\rvert$, $\lvert^{+}_{(yz)}\ ^{+}_{(xy)}\rvert$	3	$H_{av.}$ +4/5 Δ−3/2 B^1	−0.190 μm^{-1}
$\lvert^{+}_{(x^2-y^2)}\ ^{+}_{(xy)}\rvert$	1	$H_{av.}$ −1/5 Δ+15/2 B^1	−0.282 μm^{-1}
$\lvert^{+}_{(z^2)}\ ^{+}_{(yz)}\rvert$, $\lvert^{+}_{(z^2)}\ ^{+}_{(zx)}\rvert$	2	$H_{av.}$ −1/5 Δ+9/2 B^1	−0.426 μm^{-1}
$\lvert^{+}_{(x^2-y^2)}\ ^{+}_{(zx)}\rvert$, $\lvert^{+}_{(x^2-y^2)}\ ^{+}_{(yz)}\rvert$	3	$H_{av.}$ −1/5 Δ−3/2 B^1	−0.715 μm^{-1}
$\lvert^{+}_{(z^2)}\ ^{+}_{(xy)}\rvert$	4	$H_{av.}$ −1/5 Δ−9/2 B^1	−0.859 μm^{-1}
$\lvert^{+}_{(z^2)}\ ^{+}_{(x^2-y^2)}\rvert$	4	$H_{av.}$ −6/5 Δ−9/2 B^1	-1.384 μm^{-1}

[a] H_{ADF} values refer to VCl_4^-. The subconfiguration (cf. Table 1) and the spatial pair-energy class[12] define the coefficients to Δ and B^1, respectively.

Three different types of computations will be needed here, an unrestricted and a restricted SCF computation and a fixed-orbital computation. In this fixed-orbital application the ADF is used as an experimental device having an experimental uncertainty, and the parametrical results are obtained by using a least-squares averaging of the computed set of state energies. These types of computations will be described below under the headings A, C, and E.

A. Geometry Optimization by Unrestricted Self-consistent Field ADF Computation. The geometry of the ground state resulting from this computation is T_d symmetry with a V−Cl distance of 225 pm. The geometry is fixed in the following.

B. Orbital Identification by Symmetry and/or Plotting. The energy order found for the Kohn−Sham α-spin orbitals agrees with that predicted by usual heuristic qualitative MO

Table 3. Computational Results[a]

	VF_4^-	VCl_4^-	VBr_4^-	VI_4^-
$\Delta/\mu m^{-1}$ ($M_S = 1$ only)	0.693(4)	0.525(4)	0.475(3)	0.407(3)
$\Delta_{aoc}/\mu m^{-1}$	0.672	0.489	0.426	0.372
$\Delta_{exp}/\mu m^{-1}$		0.553	0.520	
$B^1/\mu m^{-1}$	0.0576(10)	0.0481(6)	0.0465(5)	0.0442(4)
$B^1_{exp}/\mu m^{-1}$		0.0494	0.0435	
Mulliken charges on V	1.46	0.63	0.78	−0.15
3d(V^{III}) fraction in t_2	79.45%	75.17%	73.50%	73.11%
3d(V^{III}) fraction in e	88.77%	84.16%	82.56%	82.56%
4p(V^{III}) fraction in t_2	6.2%	2.9%	3.0%	2.6%
V−X/pm	185	225	241	263
V spin density (ground state)	1.95	1.99	2.06	2.19
$\Delta/\mu m^{-1}$	0.675(13)	0.500(12)	0.449(12)	0.377(12)
$D/\mu m^{-1}$	0.443(11)	0.373(10)	0.361(10)	0.345(10)
$B/\mu m^{-1}$	0.0587(28)	0.0489(26)	0.0473(25)	0.0449(26)
D/B	7.55	7.61	7.65	7.67

[a] ADF-computed values for the ligand-field (Δ) and interelectronic repulsion (B^1) parameters of VX_4^- determined for each complex by a least-squares fitting of the 10 uon αα-pair ADF energies to the LFR-parametrical energy expressions. Δ_{aoc} is the KS orbital energy difference in the d^q-AOC SCF computation. The fractions refer to the contents of 3d (V^{3+}) and 4p (V^{3+}) orbitals in the partially filled shell e(π) and $t_2(\sigma,\pi)$ of the tetrahedral complexes. The spin-density on V refers to the net number of spin-up electrons in the partially filled shell obtained from the unrestricted calculation. The last four rows are the results of using all possible values of M_S (45 Slater determinants). The parameter used besides B and Δ is Jørgensen's spin-pairing energy parameter D (a linear combination of Racah's parameters B and C).[29]

considerations. The highest-energy nonempty set of orbitals is singly occupied, a SOMO set, these orbitals carrying the two electrons of the partially filled shell being of eα (T_d) symmetry type. The lowest-energy unoccupied orbital set, the LUMO set, consists of the three orbitals of $t_2\alpha$ (T_d) symmetry type. These frontier e and t_2 orbitals identify the partially filled shell, and their restricted counterparts will be identifiable as the perturbed d orbitals of ligand-field theory to be defined within the ADF by the restricted computation of step C. These orbitals will be used to build up all the states of the characterizing d^2 ligand-field configuration of the present paper. The orbital picture $e^2t_2^0$ with two electrons in the partially filled shell is in a strong qualitative sense in agreement with ligand-field theory. (This subconfiguration implies that the ligand-field oxidation state of vanadium is III, that is, equal to the conventional formal oxidation number, which forms the basis for the classification of vanadium chemistry.[15,16])

The ADF-computational result then provides a quantitative measure of the concordance with ligand-field theory in that the noninteger difference between the electronic charges of α and β electrons on vanadium is found by Mulliken population analysis to be close to 2 (cf. Table 3). Thus, the integrated, uncompensated spin on vanadium corresponding to two electrons may be taken as a probe of the ligand-field oxidation state. This fact has been noted earlier[21] for the much more covalent d^1 system, $CrN(CN)_5^{3-}$.

C. An Average-of-Configuration Computation (d^q-AOC). The d^q-AOC computation is a restricted SCF-ADF computation using appropriate frontier orbitals to represent the partially filled shell. The occupation numbers here are fractional. Described in subconfiguration form, they correspond to the averaged configuration $e^{4/5}t_2^{6/5}$ of the d^2 system. One may describe the situation as one of collecting together the incommensurable orbitals of e(T_d) and $t_2(T_d)$ symmetries into a single set of pseudo-spherical parentage. The two electrons are in the d^q-AOC computation evenly distributed upon the 10 spin orbitals of the partially filled shell whose main parentage is d orbitals with α and β spins. Thereby the electronic density and the potential created by this density obtain tetrahedral symmetry so that the eigenorbitals belong to symmetry species (irreducible representations) of the T_d point group. Thus the d^q-AOC computation defines all the KS-DFT orbitals and in particular those of the partially filled shell. This d^q-AOC-SCF computation is the backbone of the ligand-field mimicking process. Moreover, for a particular complex, this is the only SCF computation required to mimic the ligand-field modeling. The orbitals provided by the d^q-AOC computation remain fixed (frozen) during the ligand-field mimicking process. Almost as a gift, the Kohn−Sham orbital energy difference between the e(T_d) and $t_2(T_d)$ orbitals of the d^q-AOC computation turns out to agree numerically with the ligand-field one-electron energy difference obtained by the mimicking process (confer point E and Table 3). The total energy of the d^q-AOC computation serves in a ligand-field context as an external zero point of energy, which normally would be considered not to belong to the semiempirical model world of ligand fields, whose concern is only energy differences.[17] However, this zero point turns out to be more interesting than expected (cf. appendix to ref 12). Finally, the d^q AOC computation corroborates all the usual qualitative molecular orbital interpretations of the ligand-field model.

The d^q-AOC computation, which is molecular, is as analogous as possible to the atomic "average of configuration" computation, "AOC", recommended by the authors of the ADF as a starting point for computations[22,23] on atomic fragments. We used the AOC in finding the parameters of the SCS model for atomic d^q systems.[12] Our present averaging of the partially filled shell configuration is analogous to that suggested by Daul[11b,13] and by the authors of the ADF[22,23] for configurations (subconfigurations in a ligand-field context) as, for example, et_2^5. However, the present averaging over the whole partially filled shell provides the closest possible approach to the parametrical d^q model of the ligand field, which is characterized by the condition that the interelectronic repulsion is parametrized as if it had spherical symmetry, that is, by the Slater−Condon−Shortley model, while the ligand field itself is treated as having its proper symmetry, for example for VCl_4^-, the symmetry T_d. The question has always been: How good can such an inhomogeneous model be? However, there has never been a real choice for the model that was simultaneously required to be semiempirical: while the spherical model of repulsion on d^q required two energy-difference

(21) Bendix, J.; Deeth, R. J.; Weyhermüller, T.; Bill, E.; Wieghardt, K. *Inorg. Chem.* **2000**, *39*, 930.

(22) Baerends, E. J.; Branchadell, V.; Sodupe, M. *Chem. Phys. Lett.* **1997**, *265*, 481.

(23) *ADF program system, Theory*, release 2002; Vrije Universiteit: Amsterdam, 2002.

parameters, this number would have been 9 (an unattainable number of empirical parameters) for the cubic model.[3,24]

D. Selection and Use of a Complete Set of d^2 States Representative of VCl_4^-. In this paper we restrict ourselves to the 10 αα states, which form the complete set of states that have $M_S = 1$. These states can be taken to represent all the spatial combinations of the highest spin multiplicity $S = 1$ associated with the d^2 configuration of VCl_4^-. There is a 1:1 relationship between each such state and a pair of different orbitals. In the ADF, we use a state defined by attributing occupation numbers of unity to both of its two d-parentage orbitals.[12] In the LFR the associated state is a Slater determinant in the corresponding d orbitals perturbed by the chemical bonding. Thereby a 1:1 relationship between the ADF and the LFR states is established.

The Slater determinants in all the 10 possible pairs of the five different α spin orbitals of e(T_d) and t_2(T_d) spatial symmetries make up all the αα determinants of the tetrahedral strong-field subconfigurations. The ADF allows the orbitals and thereby the determinants to remain being individually identifiable by their symmetry types, that is, the standard components of the irreducible representations of the tetrahedral point group. This standard refers to the groups $T_d \supset D_2$ and was defined by Griffith[3] for the hierarchy $O_h \supset D_{4h} \supset D_{2h}$. (In fact the hierarchy used was $O_h \supset (D_{4h}) \supset D_{2h}$, the parentheses referring to group-theoretical sign details that are irrelevant here.) Important for the use with KS-DFT is the choice of real orbitals, whose squares are able to cope with spatial symmetry requirements as opposed to the absolute squares of the corresponding complex orbitals.[12] Fortunately, the most common set of real d orbitals simultaneously belong to the hierarchies

$$O_h \supset D_{4h} \supset D_{2h} \tag{5}$$

and

$$D_{\infty h} \supset D_{4h} \supset D_{2h} \tag{6}$$

and can be used to generate the standards referred to.[25]

E. ADF Computation of the Energies To Be Associated with the 10 Pairs of α Spin Orbitals. As our inputs to the ADF we use occupation numbers of the KS spin orbitals whose orbital part is real (real spin orbitals). In order to match a Slater determinant, these numbers have to be equal to unity for the orbitals of the determinant and zero for all the remaining spin orbitals. We shall write the pairs with unity occupation numbers (uon) as, for example, (e:z^2,α)(t_2:yz,α) corresponding to the Slater determinant

$$\begin{vmatrix} + & + \\ (z^2)(yz) \end{vmatrix}$$

The energies computed by the ADF for orbital occupation schemes with unity occupation numbers can be assumed to represent the total energies in terms of expectation values[12] for the states described by the corresponding Slater determinants,[9,10] these energies being measured relative to the energy associated with the d^q-AOC computation.

Among the 10 pairs of α spin orbitals, the contribution to the electronic density arising from the partially filled shell has full tetrahedral symmetry only in the case of the pair (e:z^2,α)(e:x^2-y^2,α), which corresponds to the Slater determinant

$$\begin{vmatrix} + & + \\ (z^2)(x^2-y^2) \end{vmatrix}$$

$^3A_2$(T_d). The densities of all the other αα-pairs have lower symmetries and associated contributions to the effective potential, also of lower symmetry. For this reason we cannot impose tetrahedral symmetry upon our computations for all the determinants. However, D_2 symmetry is used as a common denominator for all the 10 Slater determinants. (The computations are speeded up about four times by taking advantage of the symmetry facility of the ADF; in tetrahedral symmetry, all the individual orbitals, and thereby all the determinants, belong to symmetry species of the point group D_2. This means that the electron density and the associated effective potentials of the uon αα-pairs belong to the unit representation of D_2.)

One ADF computation is now performed for each of the determinants using the fixed orbitals from the d^q-AOC computation.

At this stage we have obtained energy values for all the 10 completely defined $M_S = 1$ states of the partially filled shell embodied in our complex VCl_4^- or any of its homologues with the other halides. These energies are not eigenenergies. Through the ligand-field mimicking process, they correspond to diagonal elements of the strong-field Hamiltonian matrix. The set of energies contains sufficient parametrical information to allow also the nondiagonal elements to be determined. Thus, the whole ligand-field energy matrix and thereby its eigenvalues may be computed.

The two final steps are a ligand-field step (F) and a comparison step (G) in which 10 linear equations are set up to determine the computed empirical parameters of the parametrical d^q model for highest spin multiplicity.

F. Energies in the Ligand-Field Parametrization. The conventional energy diagram (Orgel diagram[26]) of Figure 1 illustrates the ligand-field description of tetrahedral d^2 complexes for the higher spin multiplicity. In the weak-field limit the energies of ^3P and ^3F are not those of the gaseous ion, but rather refer to the nephelauxetically modified atomic states. $\Delta = \infty$, that is, the strong-field limit, refers to the pure strong-field configurations, which are reached asymptotically. The intercept of the tangent of any state graph with the ordinate axis expresses the interelectronic repulsion of that state at the abscissa in question. This intercept is invariably ^3F for $^3A_2$ and $^3T_2$ but changes dramatically[27] with Δ for the two $^3T_1$ states. Seen from the weak-field side, ^3P

(24) Daul, C.; Goursot, A. *Int. J. Quantum Chem.* **1986**, *29*, 779.
(25) (a) Harnung, S. E.; Schäffer, C. E. *Struct. Bonding (Berlin)* **1972**, *12*, 201. (b) Harnung, S. E.; Schäffer, C. E. *Ibid*. **1972**, *12*, 257.
(26) Orgel, L. E. *J. Chem. Phys.* **1955**, *23*, 1004.
(27) Jensen, G. S.; Brorson, M.; Schäffer, C. E. *J. Chem. Educ.* **1986**, *63*, 387.

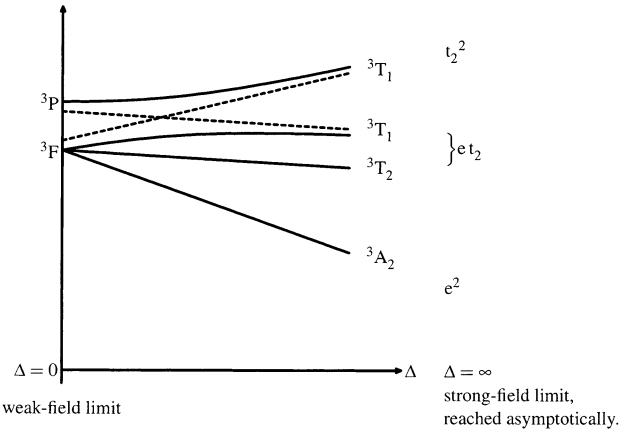

Figure 1. Ligand-field energy diagram (Orgel diagram[26]) for tetrahedral d^2 complexes showing the triplets only. In the expanded radial function model,[4c] or, with a more specific name,[27] the parametrical d^2 model, $^3A_2$ and $^3T_2$ have pure ^3F parentages. However, ^3F and ^3P are mixed in the $^3T_1$ multiplets (unless Δ is zero; cf. text and Table 1). The $^3T_1$ asymptotes have been given as dotted lines whose crossing point corresponds 50% mixing of t_2^2 and et_2.

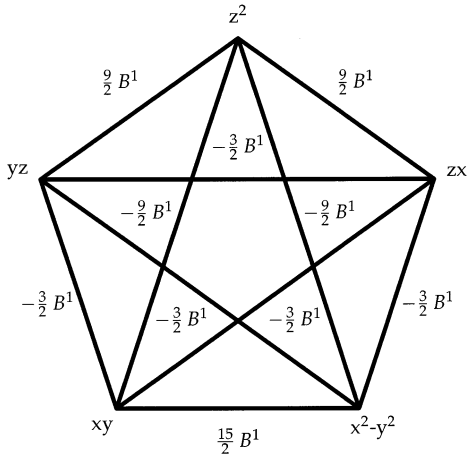

Figure 2. Pair-interaction energies between the standard real d orbitals with α spin. Energies are expressed in the Racah parameter B^1 where the suffix is our addition to emphasize that we are here concerned with $M_S = S = 1$ only. This figure illustrates the spatial energy classes[12] of Table 2.

and ^3F become mixed beyond 50% across the diagram. Seen from the strong-field side, the $^3T_1$ states of the subconfigurations t_2^2 and et_2 become mixed more than 50%. In other words, the noncrossing region is traversed (cf. Figure 1). The strong-field side, which represents the relevant view in this KS-DFT context, is illustrated in Table 1, which shows the parametrical expressions of the most pertinent asymptotes. These expressions correspond to our ADF-computed energies.

Figure 2 illustrates the pair interaction energies of the αα pairs of real spin orbitals. The pair interaction $\kappa(yz,zx)$, for example, is equal to the difference between the Coulomb integral and the exchange integral associated with the two orbitals. The expectation value of the repulsion energy is expressed in the parameter B^1. In decreasing energy order,[12] we have four spatial pair-energy classes that may be D_∞-labeled as $\delta\delta$, $\sigma\pi$, $\pi\pi$ or $\pi\delta$, and $\sigma\delta$. $\pi\pi$ and $\pi\delta$ fall in the same class because of the high symmetry inherent in the d orbitals as expressed in eqs 5 and 6. Clearly, the $\pi\pi(D_\infty)$ pair of the Slater determinant $|(yz)(zx)|$ and the $\pi\delta(D_\infty)$ pair of $|(yz)(xy)|$ must have the same energy with the repulsion operator, because $1/r_{12}$ is an R_{3i}-symmetrical operator. We are now able to use H_{av}, B^1, and Δ to express the expectation values of the energies of the parametrical d^2 model with respect to all our strong-field Slater determinants.

G. Ten Linear Equations in H_{av}, B^1, and Δ. We now use the 1:1 relationship between the uon αα-pairs of real spin orbitals of the ADF and the strong-field determinants of LFR.[12] The ADF energies of step E can be uniquely associated with the parametrical strong-field expressions of step F. Thus the partially filled shell fixed-orbital uon energies are set up in a diagonal matrix, $\mathbf{H}_{ADF}^{diag.uon}$, and the elements are identified with the diagonal elements of the strong-field energy matrix $\mathbf{H}_{LFR}^{diag.sf}$ of the parametrical d^2 model, and by juxtaposition and equalization of these two matrices, we obtain 10 linear equations

$$\mathbf{H}_{ADF}^{diag.uon} \simeq \mathbf{H}_{LFR}^{diag.\ sf} \tag{7}$$

where

$$\mathbf{H}_{LFR}^{diag.\ sf} = H_{av}\mathbf{1} + B^1\mathbf{Q}_{B^1}^{diag.sf} + \Delta\mathbf{Q}_{\Delta}^{diag.sf} \tag{8}$$

involves the three standard parameters H_{av}, B^1, and Δ of the LFR, **1** being the 10×10 unit matrix.

It should be noted that $\mathbf{Q}_{\Delta}^{sf}$ is already diagonal, that is,

$$\mathbf{Q}_{\Delta}^{sf} = \mathbf{Q}_{\Delta}^{diag.sf} \tag{9}$$

The results for VCl_4^- are collected together in Table 2. The numbers in the table are the diagonal elements of the symmetry-determined matrices **1**, $\mathbf{Q}_{B^1}^{sf}$, and $\mathbf{Q}_{\Delta}^{sf}$.

The rows of Table 2 are ordered in terms of LFR strong-field coefficients, the ligand field being given a higher priority than the repulsion. The four rows in the middle belong to the same strong-field subconfiguration et_2 and have the repulsion energies characteristic of the four spatial pair-energy classes (Figure 2). It is noteworthy that this way of fixing the order of priorities on the basis of LFR parameter coefficients results in an ordering also of the ADF energies. The relative importance of the ligand-field and repulsion terms will be further discussed in section 4.

Once the symmetry has been taken care of, the 10 pieces of ($M_S = 1$)-states provide six pieces of independent ADF computational information to determine the three parameters H_{av}, B^1, and Δ (Table 2). This determination has been done by the linear least squares procedure to obtain the parametric results of Table 3.

4. Comparison of the Way of Focusing upon d^2 States by Our KS-DFT Approach and by the Semiempirical Ligand-Field Approach

KS-DFT has the limitation that it does not allow the computation of the energy quantities that correspond to the nondiagonal elements of the Hamiltonian. By our assumptions, these "nondiagonal elements of the ADF" are implied, however, by the more general form of eq 7, which may be

written as

$$\mathbf{H}_{\mathrm{ADF}}^{\mathrm{diag.uon}} + \mathbf{H}_{\mathrm{ADF}}^{\mathrm{nondiag}} = \mathbf{H}_{\mathrm{ADF}} \simeq \boldsymbol{H}_{\mathrm{LFR}}^{\mathrm{sf}} \tag{10}$$

where the first term is the diagonal matrix that contains the energies obtained by the uon computation of the ADF, and where the right-hand side is

$$\mathbf{H}_{\mathrm{LFR}}^{\mathrm{sf}} = H_{\mathrm{av}}[^3\mathrm{P}^3\mathrm{F}]\mathbf{1} + B^1\mathbf{Q}_{B^1}^{\mathrm{sf}} + \Delta\mathbf{Q}_{\Delta}^{\mathrm{sf}} \tag{11}$$

By use of eqs 7−11 we obtain a definition of the nondiagonal elements of the ADF

$$\mathbf{H}_{\mathrm{ADF}}^{\mathrm{nondiag}} \equiv \mathbf{H}_{\mathrm{LFR}}^{\mathrm{nondiag.sf}} = B^1\mathbf{Q}_{B^1}^{\mathrm{nondiag.sf}} \tag{12}$$

where $\mathbf{Q}_{B^1}^{\mathrm{sf}}$, and thereby its nondiagonal part $\mathbf{Q}_{B^1}^{\mathrm{nondiag.sf}}$, is symmetry determined. The only difference between the two strong-field equations 7 and 10 is the nondiagonal elements stemming from $B^1\mathbf{Q}_{B^1}^{\mathrm{sf}}$. These elements are a necessary consequence of the LFR model, and, by the assumption of a general 1:1 relationship between the ADF and LFR models, they are implied also for the ADF, which is thereby adapted to an energy-matrix form allowing the computation of its eigenenergies (and eigenfunctions) under the constraints imposed upon the Kohn−Sham DFT by the d^q-AOC computation and by the LFR modeling.

The formalism described here also allows a norm-square comparison of the full semiempirical ligand-field description of $[VCl_4]^-$ and the present uon KS-DFT description, which represents the diagonal part of the strong-field matrices, that is, the tetrahedral strong-field approximation, in which the ligand field, but not the repulsion, is diagonal. The comparison is made by using the matrix equation

$$\bar{\mathbf{H}}_{\mathrm{LFR}}^{\mathrm{sf}} = B^1\mathbf{Q}_{B^1}^{\mathrm{sf}} + \Delta\mathbf{Q}_{\Delta}^{\mathrm{sf}} = B^1\mathbf{Q}_{B^1}^{\mathrm{diag.sf}} + B^1\mathbf{Q}_{B^1}^{\mathrm{nondiag.sf}} + \Delta\mathbf{Q}_{\Delta}^{\mathrm{sf}} \tag{13}$$

The ligand-field matrix $\Delta\mathbf{Q}_{\Delta}^{\mathrm{sf}}$ is orthogonal to both the nondiagonal and the diagonal part of the repulsion matrix; in turn these two latter matrices are mutually orthogonal by the definition of eq 3. Therefore, if the two equalities of eq 13 are thought of as two vector descriptions of $\bar{\mathbf{H}}_{\mathrm{LFR}}^{\mathrm{sf}}$ (in the sense described in section 2), then the vectors within each of these descriptions are mutually orthogonal. The length of such a vector is the square root of the norm square of the corresponding matrix, i.e., the parameter times the square root of the norm square of its coefficient matrix.

Using eq 3 the norm square of the diagonal matrix $\mathbf{Q}_{\Delta}^{\mathrm{sf}}$ can be found from the coefficients to Δ of Table 2,

$$\langle\hat{Q}_{\Delta}|\hat{Q}_{\Delta}\rangle = \langle\mathbf{Q}_{\Delta}^{\mathrm{sf}}|\mathbf{Q}_{\Delta}^{\mathrm{sf}}\rangle = \langle\mathbf{Q}_{\Delta}^{\mathrm{diag.sf}}|\mathbf{Q}_{\Delta}^{\mathrm{diag.sf}}\rangle = 18/5 \tag{14}$$

and the norm square of $\mathbf{Q}_{B^1}^{\mathrm{diag.sf}}$ can be found from the coefficients to B^1 of Table 2,

$$\langle\mathbf{Q}_{B^1}^{\mathrm{diag.sf}}|\mathbf{Q}_{B^1}^{\mathrm{diag.sf}}\rangle = 297/2 \tag{15}$$

However, the operator $\hat{Q}_{B^1}$ is diagonal in the weak-field basis only and its norm square is accordingly

$$\langle\hat{Q}_{B^1}|\hat{Q}_{B^1}\rangle = \langle\mathbf{Q}_{B^1}^{\mathrm{wf}}|\mathbf{Q}_{B^1}^{\mathrm{wf}}\rangle = \langle\mathbf{Q}_{B^1}^{\mathrm{diag.wf}}|\mathbf{Q}_{B^1}^{\mathrm{diag.wf}}\rangle = (21/2)^2 \times 3 + (9/2)^2 \times 7 = 945/2 \tag{16}$$

(cf. illustration b).

The norm-square of $\hat{Q}_{B^1}$ may alternatively be written as

$$\langle\hat{Q}_{B^1}|\hat{Q}_{B^1}\rangle = \langle\mathbf{Q}_{B^1}^{\mathrm{diag.sf}}|\mathbf{Q}_{B^1}^{\mathrm{diag.sf}}\rangle + \langle\mathbf{Q}_{B^1}^{\mathrm{nondiag.sf}}|\mathbf{Q}_{B^1}^{\mathrm{nondiag.sf}}\rangle = 945/2 \tag{17}$$

Combining eqs 15 and 17 one concludes that only 297/945 = 11/35 of the information about $\hat{Q}_{B^1}$ lies in the strong-field diagonal, which is that taken from ligand-field theory in order to compute B^1 and thereby obtain the nondiagonal elements of KS-DFT within the partially filled shell (cf. eq 12) and thereby the computed eigenenergies.

Using the norm squares of the coefficient operators together with the computed parameters for VCl_4^-, we have depicted the vectors corresponding to eqs 10 and 13 in Figure 3.

The comparison of $\hat{H}_{\mathrm{LF}}$ and $\hat{H}_{\mathrm{R}}$ in the full matrix description and in the strong-field approximation is interesting also in terms of sum-square splittings. By using the Δ value for VCl_4^- from Table 3 with eq 14, one obtains

$$\mathrm{SSS}_{\Delta} = \langle\hat{Q}_{\Delta}|\hat{Q}_{\Delta}\rangle\Delta^2 = \langle\mathbf{Q}_{\Delta}^{\mathrm{sf}}|\mathbf{Q}_{\Delta}^{\mathrm{sf}}\rangle\Delta^2 = (18/5)(0.523\mu\mathrm{m}^{-1})^2 = 0.9847\mu\mathrm{m}^{-2} \tag{18}$$

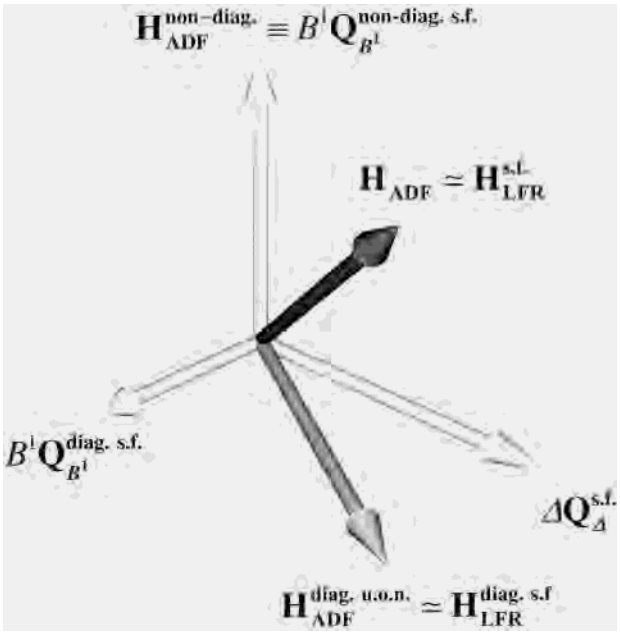

Figure 3. Vectorial representation of the connection between our ADF and LFR descriptions of the energy splitting of the $M_S = 1$ states of the d^2 configuration of VCl_4^-. The strong-field matrices are represented by three mutually orthogonal vectors, which add up to the vector representing $\mathbf{H}_{\mathrm{LFR}}^{\mathrm{sf}}$. The horizontal vectors represent $B^1\mathbf{Q}_{B^1}^{\mathrm{diag.sf}}$ and $\Delta\mathbf{Q}_{\Delta}^{\mathrm{sf}}$ and the vertical one $B^1\mathbf{Q}_{B^1}^{\mathrm{nondiag.sf}}$. The two former ones are those involved in establishing the 10 linear equations connecting ADF and LFR (cf. eq 7). $\mathbf{Q}_{B^1}^{\mathrm{nondiag.sf}}$ is symmetry determined, and, therefore, once the parameter B^1 has been obtained by solution of these equations, the matrix $B^1\mathbf{Q}_{B^1}^{\mathrm{nondiag.sf}}$ is known as well and thus the complete energy matrix. By the assumption of a general 1:1 relationship between the ADF and the LFR, an ADF energy matrix can now be defined, and thus the eigenenergies of the ADF be calculated. Note that $\mathbf{H}_{\mathrm{ADF}}^{\mathrm{diag.uon}}$ is computed directly by the ADF while $\mathbf{H}_{\mathrm{ADF}}^{\mathrm{nondiag}}$ is derived from $\mathbf{H}_{\mathrm{ADF}}^{\mathrm{diag.uon}}$ by the use of the 1:1 link (cf. also eqs 10 and 12).

and with eq 15, one obtains

$$SSS_{B^1,\text{diagonal}} = \langle \mathbf{Q}^{\text{diag.sf}}_{B^1} | \mathbf{Q}^{\text{diag.sf}}_{B^1} \rangle (B^1)^2 = (297/2)(0.0479 \mu\text{m}^{-1})^2 = 0.3407 \mu\text{m}^{-2} \quad (19)$$

From eqs 18 and 19 one calculates a ratio of 1.7 between the corresponding root-mean-square splittings, thereby obtaining a qualitative understanding of why the priority, LF before R, rationalizes the ADF energy order of Table 2. These results should be compared with

$$SSS_{B^1} = \langle \hat{Q}_{B^1} | \hat{Q}_{B^1} \rangle (B^1)^2 = \langle \mathbf{Q}^{\text{wf}}_{B^1} | \mathbf{Q}^{\text{wf}}_{B^1} \rangle (B^1)^2 = (945/2)(0.0479\, \mu\text{m}^{-1})^2 = 1.0841\, \mu\text{m}^{-2} \quad (20)$$

obtained from eq 17, showing that repulsion is the (slightly) dominating term when the full LFR model is used. With the equivalence between the ADF and the LFR, the comparison of eqs 18−20 also becomes relevant for the ADF (cf. Figure 3) by quantifying how this essentially one-electron model overemphasizes the one-electron parameter Δ of eq 18 over the two-electron parameter B^1.

5. Results and Discussion

The computed values for the parameter sets $\{\Delta, B^1\}$ given in Table 3 may be compared with the experimental values[14c] based upon the reflection spectra of $[(C_6H_5)_4As]VCl_4$ and $[(C_2H_5)_4N]VBr_4$. The parameter sets based upon these data[14c] were given as $\Delta = 0.553\ \mu\text{m}^{-1}$ and $B^1 = 0.0494\ \mu\text{m}^{-1}$ for VCl_4^- and $\Delta = 0.520\ \mu\text{m}^{-1}$ and $B^1 = 0.0435\ \mu\text{m}^{-1}$ for VBr_4^-.

The computed and experimental results for Δ and B^1 are remarkably close (Table 3). However, before evaluating the results, it is important to clarify at least a couple of the limitations of ligand-field theory. First of all, the experiments, which this model theory is concerned with, can only be partially accounted for. The experiments involve vibronic optical transitions, often represented by two or three broad bands, each with a band maximum, width, and intensity. The theory is electronic only, and usually energy differences between certain of its eigenvalues are identified with positions of observed band maxima. The theory needs various extensions in order to be able to provide as much as a qualitative idea about the other features of the experimental spectra. The simplest connection between experiment and model theory regarding eigenvalues is an association through the idea of vertical transitions. This is what we have aimed at mimicking by our fixed nuclei and fixed orbitals DFT model.

With all this conceptual complexity in mind, it is remarkable that the Δ value is reproduced so well in the orbital energy difference obtained from the d^q-AOC-SCF-ADF computation as well as in the least-squares ADF results based upon unity occupation numbers for fixed d^q-AOC orbitals (cf. heading C of section 2 and Table 3). It is at least equally remarkable that the nephelauxetic phenomenon, which parametrically could be considered to be an experimental fact,[12] in the present computation is not only parametrically reproduced but also associated with the characteristic charge transfer[17a] from the ligands to the central ion. This charge transfer was originally with great chemical satisfaction taken as the phenomenon's qualitative explanation, which was used to name it: an expansion of the partially filled shell caused by the screening from the central ion nuclear charge by the coordinative covalency, here charge transfer from the chloride ligands to the metal ion V^{3+} (central field covalency[4c]). Here, using a Mulliken population analysis as a basis, the charge carried on the vanadium center in the restricted d^q-AOC-SCF computation for VCl_4^- is found to be 0.63 to be compared with the formal charge of 3. In this analysis the chloride ions have accordingly collectively transferred a negative charge of 2.37 units to the V^{3+} ion in the bonding process. For comparison the integrated net spin-density on V is close to 2, i.e., the number of unpaired electrons (cf. Table 3 and section 3B).

Jørgensen, in discussing the nephelauxetic phenomenon, gave an additional explanation, which he called *symmetry-restricted* covalency. In an LCAO description, this is the fact that the eigenorbitals carrying the partially filled shell have been diluted as regards their contents of central ion d orbitals (cf. Table 3). The d−d repulsions were then assumed to make up the dominating terms in the repulsion between the electrons in the eigenorbitals. This assumption was used successfully by Jørgensen to establish his idea of optical electronegativities[28] whose numerical values were obtained from observed electron transfer spectra, corrected for repulsion by observed spin-pairing energy[29] expressions obtained from ligand-field spectra. This assumption was also the basis for the present method of mimicking the parametrical d^q model.

The fact that the spectrochemical series (Δ series) and the nephelauxetic series (B series) are roughly invariant series spanning over all classical transition metal complexes is perhaps the most remarkable feature of ligand-field theory. Therefore, in order to try to follow up the success of our VCl_4^- and VBr_4^- computations with a broader inorganic-chemistry perspective, we have extended our calculations to a few comparable systems. In Table 3 we have added the ions VF_4^- and VI_4^-, which represent parametric extremes in both series. (It should be mentioned in this context that VBr_4^- was prepared from $[(C_2H_5)_4N]V(CH_3CN)_2Br_4$ by a heating process. It should not, therefore, worry us too much that the VF_4^- and VI_4^- ions have not yet been prepared because this may well be due to competition for available coordination space under almost all chemical conditions. For example, VF_4^- must be formed under conditions where VF_6^{3-} is a competitive alternative.)

This paper has been concerned only with the states with maximum spin-multiplicity. The parametrization of the repulsion involving the complete set of d^q states is more complex. In this case an additional repulsion parameter is required in the SCS model. This parameter can be chosen as Jørgensen's spin-pairing energy parameter D (Table 3).[29]

(28) Jørgensen, C. K. *Orbitals in Atoms and Molecules*; Academic Press: London, 1962.
(29) Jørgensen, C. K. *Modern Aspects of Ligand Field Theory*; North-Holland Publishing Company: London, 1971.

In atomic d^q ions the ratio *D/B* lies between 7.4 and 7.9 in most cases, and for atomic V^{3+}, the value $D/B = 7.6$ was found. For the VX_4^- complexes, the ADF computed values for *D* and *D/B* have been given. Experimental values for *D* are not available, but the ADF values for *D* obey the hypothesis of an invariant nephelauxetic series and the *D/B* ratios are not far from their atomic values.

The spectrochemical and the nephelauxetic series are borne out by our computational results, and, in particular, the pronounced difference between fluoride on the one hand and the three heavier halides on the other one, known from ligand-field studies as well as from chemistry, can be observed in the two series of spectral parameters. In the Mulliken charges a small irregularity occurs between chloride and bromide. The same is true for the vanadium p-electron content in the t_2 orbitals (Table 3). However, regarding the d electron delocalization covalency, the halide series is as chemically expected. For example, from the d^q-AOC-SCF computation the σ interacting t_2 orbitals are found to have 75.17% 3d character in VCl_4^- and only 73.50% in VBr_4^- where the percentages refer to the 3d orbital of the atomic fragment V^{3+}. The computational result is that the degrees of covalency of the V^{III}−chloride and V^{III}−bromide bonds are not very different, but the example also illustrates that the concept of covalency cannot be quantified one-dimensionally. In actual fact, there are ADF standard basis sets that reverse Cl^- and Br^- in the nephelauxetic series. However, F^- and I^- are invariably placed on the wings (the position of F^- being isolated from the other three halides).

6. Conclusions

The present simple KS-DFT modeling provides an independent approach to the parameter world of ligand-field theory. This theory's qualitative molecular orbital interpretation is completely confirmed by the d^q-AOC computation. Here this statement has been confirmed for the VX_4^- (X = F, Cl, Br, I) systems, but it is yet to be seen how general its validity is. The 1:1 mimicking of ligand-field theory by KS-DFT allows the KS-DFT energies to be set up in an energy matrix that can be diagonalized so as to obtain the KS-DFT eigenstates.

We find our results unexpected for three different reasons related to the way the results are obtained.

1. The method is based on a unification of the e and t_2 molecular orbitals of the partially filled shell, which would become commensurable by suppression of their molecular character and then converge into a d^q configuration, $e^{2q/5}t_2^{3q/5} \rightarrow d^q$.

2. The method involves Kohn−Sham spin orbitals whose spatial factors must be real. They remain fixed (frozen) all through the ligand-field-theory mimicking process, fixed orbitals being a prerequisite for this process.

3. In spite of the fact that the e and t_2 eigenorbitals are different with respect to ligand orbital contents, the Slater−Condon−Shortley parametrization of their repulsion energies is successful for all VX_4^- systems.

Acknowledgment. J.B. acknowledges support (SNF-#001266) from the Danish Research Council.

IC0262233